

Rheokinetic study on homogeneous polymer reactions in melt state under strong flow field

Ji Zhou, Wei Yu*, Chixing Zhou

Advanced Rheology Institute, Department of Polymer Science and Engineering, Shanghai Jiao Tong University, Shanghai 200240, People's Republic of China

ARTICLE INFO

Article history:

Received 4 January 2009
Received in revised form
28 May 2009
Accepted 30 June 2009
Available online 8 July 2009

Keywords:

Rheokinetic
Homogeneous reaction
Strong flow field

ABSTRACT

A branch reaction of high density polyethylene initiated by Dicumyl peroxide in an internal batch mixer was used to investigate the rheokinetics on homogeneous polymer reactions in melt state under strong flow environment. The effect of shear strength on the reaction process was focused. A real conversion of reaction was put forward from the rheological measurement, i.e., the torque of mixer. A comparison of the reaction conversion from experiment and the chemical kinetic model gave a flow dependent combination rate parameter. A rheokinetic equation was therefore obtained which is in a good accordance with the theoretical prediction by Fredrickson and Leibler [4]. The rheokinetic equation was further verified by a simplified nonisothermal two-dimensional numerical simulation which incorporates macro-convection effect.

© 2009 Elsevier Ltd. All rights reserved.

1. Introduction

It is well known that the chemical reactions occurring in the reactive processing of polymers are often composed of reactions between polymer chains. The progress of reactions is usually controlled by the diffusion rate of mass transfer rather than the kinetics of chemical bonding mechanisms [1], which is known as the diffusion-controlled reaction. Diffusion-controlled reactions are often attributed to the high viscosity and the reduced mobility of reactive sites, particularly when such sites are tethered to polymer chains in melt state. In principle, any factor that affects the motion of reactive species can change the kinetics of reactions. If the reactive species are simple fluids or solids, the problem is much simple since the diffusion coefficient is only determined by the viscosity of matrix. Flow should have no obvious effect on the reaction kinetics under this condition. When the reactive species are polymer chains especially in melt, its diffusion is greatly dependent on the chain conformation, which is related to the relaxation behavior of the chain and the applied flow. Moreover, the reaction mechanism may be changed by the flow dependent diffusion process [2]. Understanding the effect of flow on the polymer–polymer reaction in melt state not only helps to optimize the polymer reactive processing, but can also serve as a justification of the dynamical theory of polymer chain motion, which makes this problem both industrially important and scientifically meaningful.

For a homogenous system under quiescent condition, de Gennes [3] once investigated diffusion-controlled processes where the reacting groups were attached to polymer chains, both entangled and non-entangled. Scaling relationships between reaction rate parameter k and degree of polymerization N have been suggested. The rate parameter scales with degree of polymerization were $k \sim N^{-1/2}$ for non-entangled chains and $k \sim N^{-3/2}$ for entangled ones. Later, Fredrickson and Leibler [4] extended de Gennes work to include the effect of steady linear flow. Different scaling relations between the reaction rate parameter and the Deborah number have been suggested, depending on the entanglement state and the elasticity of polymer chains. It is suggested that

$$k \propto \begin{cases} D_0 R (1 + 0.8068 De^{1/2}) & (De \ll 1) & (1.a) \\ D_0 R \frac{De}{\ln De} & (1 \ll De \ll \tau_d / \tau_R \approx N) & (1.b) \\ \dot{\gamma}^{1/3} & (De \gg \tau_d / \tau_e \approx b^6 N^3) & (1.c) \end{cases}$$

where $De = \tau_d \dot{\gamma}$ is Deborah number, τ_d is the disentanglement time of reptation model, $\dot{\gamma}$ is the shear rate, τ_R is the Rouse relaxation time, τ_e is the time for a Rouse displacement of order a tube diameter, D_0 is the reactive chain center-of-mass diffusion coefficient, R is the chain radius of gyration, b is the statistical segment length and N denotes the degree of polymerization. It is shown by Eq. (1) that flow will accelerate the polymer–polymer reaction. However, important assumptions have been made when obtaining this result. Firstly, Eq. (1) gives a long time reaction rate constant,

* Corresponding author. Tel.: +86 21 54743275; fax: +86 21 54741297.
E-mail address: wyu@sjtu.edu.cn (W. Yu).

although the rate parameter k is probably time dependent. Secondly, chain length distribution has not been considered, and the reaction sites are assumed to be on the end of polymer chain. Thirdly, Eq. (1) is based on the constant material properties throughout the reactions. In fact, the properties of polymers, such as viscosity and relaxation time, would change a great deal during the reaction process, which will further affect the kinetics of different reactions. Therefore, the experimental verification becomes very difficult, and the exact dependence of reaction rate on the strain rate of flow in real systems is still unclear. Other approaches have also been suggested with similar results. For example, Liu et al. [5] studied the rate parameter of diffusion-controlled polymer–polymer reaction under steady shear flow, and correlated the conformation of polymer chain with the rate parameter of reaction. A $k \sim N^{-3/2}$ scaling relation was found, which was consistent with de Gennes' scaling prediction.

Experimentally, there were some diffusion-controlled kinetic research works focusing on the curing or crosslinking [6–8] and bulk polymerization [9,10] but without flow field. Liu et al. [11] studied the influences of oscillating amplitudes on the coupling kinetics in high density polyethylene (HDPE)/peroxide reaction system, and a negative exponential expression between combination rate constant and complex viscosity of whole reactive system had been obtained. Liu et al. [12,13] also found the effect of flow on the chain scission, which turned out to be a possible approach to control the chain topology [14] during reactive processing. Although all these efforts have been made to understand the effect of flow field on the polymer–polymer reactions, quantitative result is still absent. The reasons lie in the basic principle of diffusion-controlled polymer reaction under flow field. To find an obvious effect of flow field, the Deborah number (or equivalently the strain rate for a specified polymer) should be sufficiently large, which is not readily fulfilled in a rheometric flow. While in a mixing type flow, such as in batch mixer or extruder, complex flow field and temperature distribution become a problem even though the shear rate can be much higher.

In this paper, high density polyethylene branch reaction in molten state initiated by Dicumyl peroxide (DCP) will be used to study the relationship between flow strength and reaction kinetics.

The reaction will be carried out in an internal batch mixer and a complex flow field is introduced into this research. We will present a first experimentally determined rheokinetic result for polymer–polymer reactions under entangled state.

2. Experimental

2.1. Materials

High density polyethylene (HDPE), injection molding grade M80064, with melt flow index of 8 g/10 min (190 °C, 2.16 kg, Ø2.095 mm), density of 0.964 g/cm³ and $M_w = 83\,086$ g/mol was obtained from SABIC, Saudi Arabia. Dicumyl peroxide (DCP, chemical pure, molecular weight = 270 g/mol), xylene (a mixture of *o*-, *m*- and *p*-xylene whose boiling point is about 140 °C and density, 0.87 g/cm³ at 20 °C), and acetone (chemical pure) were all purchased from Shanghai Chemicals Factory, China PR. The decomposition rate constant of DCP, k_d , is 0.003398 s⁻¹ and 0.0214 s⁻¹ at 160 °C and 180 °C and the corresponding half-life time is 204 s and 32.4 s at 160 °C and 180 °C.

2.2. Homogeneous mixing reaction in Haake internal batch mixer

We adopted the Haake internal batch mixer (Haake PolyLab OS system with an approximate volume of 70 ml, Thermo Fisher, Germany) as the reactor of radical reaction of polyethylene. The geometry of mixer is shown in Fig. 1. It has two counter-rotating triangle-like rotors with rotational speed ratio 1.25:1 (left to right). The HDPE particles and DCP powder were firstly immersed into acetone at room temperature to keep DCP dispersed evenly in body of polyethylene before mixing started and it was assumed that the acetone has volatilized thoroughly after 24 h exposure in air. A completely filled reactant system of mixer was used in our experiment, 55 g pure HDPE and DCP (0.16% pure HDPE) could make sure the mixer was fully filled. 0.16% DCP can also guarantee only a few HDPE molecular chains to react with each other and no gel formation. When the barrel of mixer was preheated to the desired processing temperature 160 °C, the raw material started to be fed into the mixer rotating at 60 rpm (rounds per minute). A

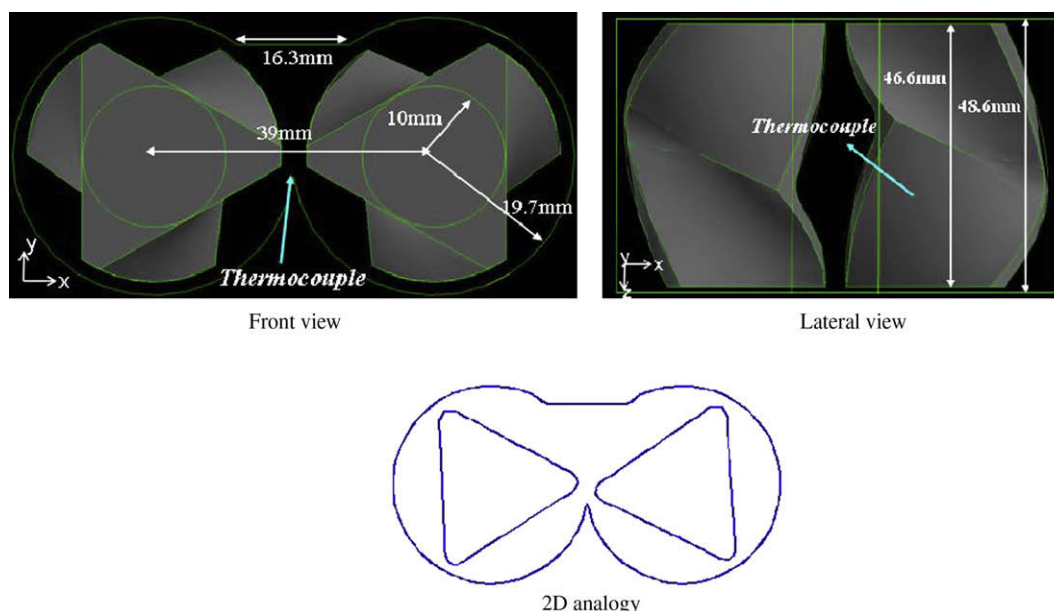


Fig. 1. Schematic illustration of Haake mixer and its simplified two-dimensional model.

thermocouple was mounted in the bottom of the mixer to measure the melt temperature (see Fig. 1) and total torque acting on the rotors was measured from transducers mounted on the shafts. When mixing started, the evolution of torque and temperature from experiment were recorded to reflect the course of polymer reaction. The effects of flow intensity on reactions were investigated by changing the rotational speeds (20 rpm, 40 rpm, 80 rpm and 100 rpm).

2.3. Product analysis and rheological measurement

The gel content of fully reacted products was measured using Soxhlet extraction cycle for 24 h with xylene as the solvent at 140 °C. It was found that the gel content of all reacted HDPEs was zero which meant that no gel (crosslinked structure) but only extended chains were formed in the reaction. In addition, a rotational rheometer, Gemini 200HR (Bohlin Instruments, UK), with two parallel plates of diameter 15 mm was used for the rheological measurements. The melt flow activation energy E_L of pure HDPE was determined to be 25.3 kJ/mol by the viscosity curve obtained from steady shear rate sweep at different temperatures. The steady shear rate sweep result of original and extended HDPE at 180 °C is given in Fig. 2, respectively. Bird–Carreau model was used to fit the rheological properties (Table 1). It can be seen that Bird–Carreau model could describe the rheological behavior of pure and reacted PE well. A dynamic frequency sweep from 0.01 to 100 rad/s on samples before and after reaction was also tested under 180 °C and 5% linear strain amplitude. The sweep results are displayed in Fig. 3. It can be seen the complex viscosity and dynamic modulus of branched PE increased greatly as compared with unreacted linear PE.

2.4. Numerical simulation method

Fluent, a finite volume method based CFD software package was also used to evaluate the flow features in the case of homogeneous mixing reaction inside Haake mixer and further to testify the derived rheokinetic equation afterwards. Correspondingly, a simplified two-dimensional (see Fig. 1) isothermal or non-isothermal model of mixer was respectively adopted for implement of above objects, and the geometric structure employed was the cross-sectional shape of mixer. In order to resolve the time-periodic changing fluid domain due to motion of the rotor boundaries, a dynamic mesh technique [15] was applied. Besides, a smoothing

Table 1

Bird–Carreau fitting parameters of linear and branched PE at 180 °C.

$\eta = \eta_0 / ([1 + (\lambda\dot{\gamma})^2]^{(1-n)/2})$	η_0 (Pa s)	λ (s)	n
Linear PE	1981.4	4.76	0.81
Branched PE	76,711.5	46.7	0.5

η_0 : zero shear viscosity; λ : relaxation time; n : power index.

and local meshing method [15] was used to update the mesh in deforming regions subject to the moving boundaries. At every moment t , the iterative process was repeated until a convergence criterion was reached. The convergence criterion used here in each time step was checked by the total relative error of velocity and mass fraction fields, which was set to be 10^{-3} .

3. Results and discussion

3.1. Kinetics of PE branch reaction initiated by DCP

To analyze the kinetics of the combination reaction of HDPE, several assumptions and simplifications are necessary:

- All the PE chains have the same linear architecture and mobility, and the architecture of original linear PE chains with molecular weight M_L will keep unchanged during reaction.
- The primary radicals produced by the initiator at certain time t will be converted to secondary macromolecular radicals completely, and it is supposed that the reactive PE chains are uniformly distributed in PE matrix before combination reaction happens.
- The reactive center of PE chain arises in the middle of PE backbone on the average and two reactive PE chains will couple to yield an extended chain which is assumed to have four-arm stars structure with average molecular weight $2M_L$ and each arm of the same average molecular weight $M_a \approx M_L/2$. Therefore, the PE melt under modification can be considered as a blend of linear chains and four-arm star chains at any time t .
- The only termination reaction is the coupling reaction between two polymer chains. The combination reaction occurs immediately and irreversibly when two reactive PE chains approach within a “capture radius”. The termination reaction by disproportionation and all the side reactions are ignored.

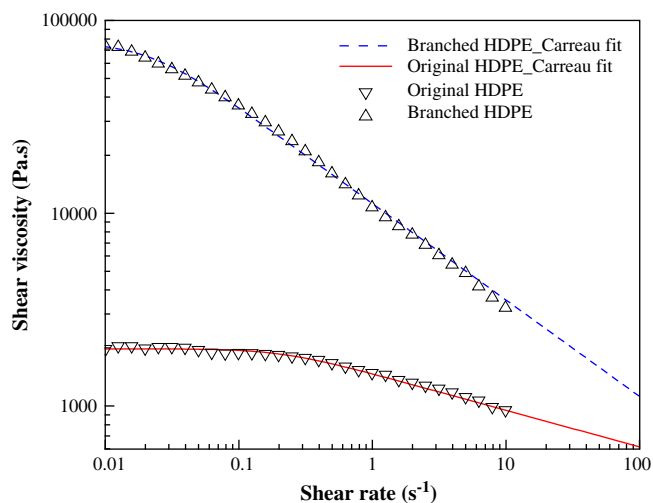


Fig. 2. Steady shear viscosity of original and branched HDPE as a function of shear rate under 180 °C.

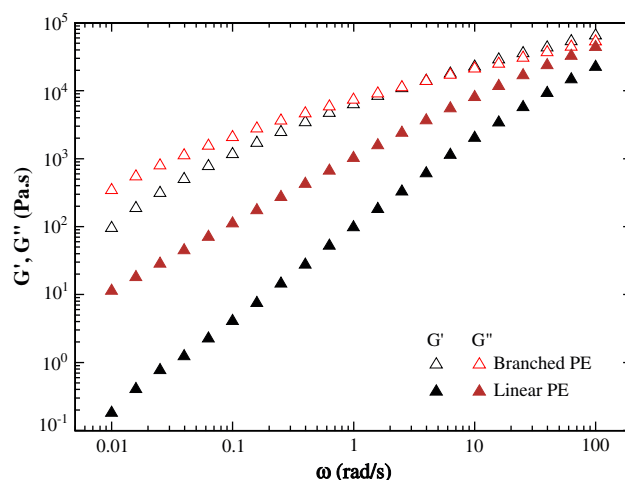


Fig. 3. Dynamic frequency sweep on linear and branched PE samples under 180 °C (strain = 5%).

Based on the above assumptions and simplifications, the mechanism of peroxide induced branch reaction of PE can be summarized as the following three steps [11]:

Step 1: initiation reaction by DCP



$$\frac{d[RO\cdot]}{dt} = -2f\frac{d[I]}{dt} = 2fk_d[I] \quad (3)$$

where $[I]$ and $[RO\cdot]$ are respectively the concentration of initiator and primary radicals at time t , and f is initiator efficiency which is assumed to be 0.5 for all processing conditions in this work. It should be noted that different flow field will lead to different initiator efficiency in fact at a high polymer concentration system. That is mainly resulted from the combining effects of abrupt increase in system viscosity (cage effect) after coupling reaction and flow induced shear thinning of it. It could be anticipated, the initiator efficiency will decrease step by step due to occurrence of higher viscosity component under quiescent condition whereas the introduction of flow field actually implies two contradictory impacts on this process. One effect is enhancing the initiator efficiency at the initial stage of reaction due to shear thinning and the other is limiting it because of the accelerated coupling reaction. As a whole, a compromising effect on initiator efficiency of flow is anticipated to be similar among all the five rotor speed cases and only $f=0.5$ is adopted here. k_d is the initiator decomposition rate constant. $[I_0] = 4.66 \text{ mol/m}^3$ is the initial concentration of initiator in the mixer.

Step 2: hydrogen abstraction and formation of macro-radicals



In this step, primary radical will attack on the polymer chain via hydrogen abstraction to generate macro-radicals. Because k_a (10^6 – 10^7 l/mol s) is usually far larger than k_d (10^{-4} – 10^{-1} s^{-1}), so it can be supposed that produced primary radicals in step 1 at time t can be transformed immediately and completely into polymer radicals in step 2. In that case, the following expression will hold:

$$[P\cdot] \approx [RO\cdot] \quad (5)$$

Step 3: termination reaction by combination of macro-radicals and formation of branching point. The termination by disproportionation and other side reactions are assumed negligible [16,17]



$$\frac{d[P\cdot]}{dt} = 2fk_d[I] - k_t[P\cdot]^2 \quad (7)$$

$$\frac{d[P-P]}{dt} = \frac{1}{2}k_t[P\cdot]^2 \quad (8)$$

where k_t is the combination rate constant and it is generally known that this step is the diffusion-controlled step.

It is known that shear flow not only affects chemical reaction but also morphology transition such as flow-induced phase separation. However, as for the branch reaction of polyethylene, there is no evidence to show the phase separation of branched chains and linear chains. Besides, nearly there were almost no differences in chemical structure of macromolecules before and after reaction, it is expected that the possibility of shear-induced phase separation in this reactive system should be very low. Therefore, only the effect of flow on the kinetic process of reaction will be considered subsequently.

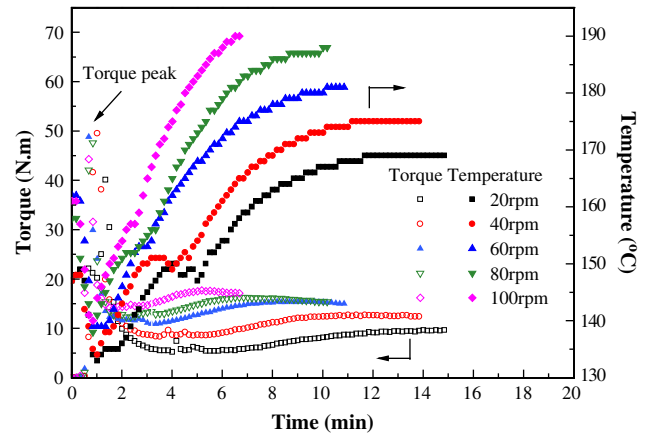


Fig. 4. Experimental curves of torque and temperature with time during branch reaction of polyethylene under different rotational speeds in Haake mixer.

3.2. Definition of reaction conversion

The typical experimental temperature and torque evolution of polyethylene with Dicumyl peroxide under processing temperature 160°C are recorded in Fig. 4. Because of quick adding raw materials into mixer, the torque peak in Fig. 4 reflected the superposition effect of feeding and molten accumulation of particles. After that, both of the torque and temperature tended to reach steady state until a certain time when a clear slope change arises in torque and temperature curves. This was attributed to the structure change of PE chains during radical reaction, which results in an increase of viscosity and then the enhanced viscous dissipation. It can be seen that the torques increased continuously with reaction time, and finally reached steady values. It was interesting to see that the reaction time (defined as the time span of rising torque) decreased with the increasing rotational speed. However, decrease of reaction time at higher rotational speed could be a result of accelerated reactions under stronger flow field or under higher temperature. Then it is necessary to differentiate these two effects to understand the rheokinetics of polymer reactions.

Firstly, to correlate the experimental torque with reaction process, the recorded instantaneous torque was considered to be proportional to the viscosity of materials at mixing time t under temperature T :

$$\tau(t, T) \propto \eta(t, T) \quad (9)$$

Such relationship has been suggested by Bousmina [18] where the proportional coefficient depends only on the geometry of the mixer. According to previous kinetic description, the melt can therefore be considered a “blend” of four components at any time t : unreacted initiator, unreacted linear polyethylene, linear polyethylene radical and branch polyethylene. The viscosity of polymers will be mostly contributed by $(1-y)$ fraction of linear polyethylene and y fraction of branch polyethylene. Here, y is mass fraction of branched chains, and increases with time t . The viscosity of polymers during reaction is assumed to obey a logarithmic addition law [19]:

$$\eta(t, T) = \eta_L(T)^{1-y(t)} \eta_B(T)^{y(t)} \quad (10)$$

where the subscripts L and B denote a linear and a branched molecule, respectively.

It is worth noting that the viscosity logarithmic mixing rule is merely an empirical one in fact and it has been tested in some miscible blends only for zero shear viscosity. Other kinds of mixing

rule can also be used such as the double reptation model [20] or some improved model [21]. All these models are suggested for zero shear viscosity. However, nonlinear dependence of viscosity on the composition makes the kinetic analysis rather difficult. Moreover, the mixing rule for miscible blends under shear flow requires the knowledge of individual chain dynamics in blends, which remains an unsolved problem at present. The experimental results of Liu et al. [22] show that the shear viscosity of blends of linear polymers will agree log-mixing rule, while deviation appears for the blends of linear and branched polymers, which is ascribed to the miscibility. So anyway, it is expected that logarithmic mixing rule can serve as an approximation for the viscosity under shear flow.

Therefore, the amount of branched chain can be obtained as:

$$y(t) = \frac{\ln[\eta(t, T)/\eta_L(T)]}{\ln[\eta_B(T)/\eta_L(T)]} \quad (11)$$

$\eta_L(T)$ and $\eta_B(T)$ are the temperature dependent viscosities of pure linear PE and pure branched PE, respectively. Therefore, the relative conversion can be calculated as:

$$\beta_r = \frac{y(t)}{y(t \rightarrow \infty)} = \frac{\ln[\eta(t, T)/\eta_L(T)]}{\ln[\eta(t \rightarrow \infty)/\eta_L(T)]} = \frac{\ln[\tau(t, T)/\tau_L(T)]}{\ln[\tau(t \rightarrow \infty)/\tau_L(T)]} \quad (12)$$

where $\tau_L(T)$ denotes the equilibrium torque of original linear PE which is a function of processing temperature and rotor speed (see Fig. 5) and $\tau(t \rightarrow \infty)$ is the equilibrium torque of reacting system when reaction finished. It can be seen that conversion definition (12) is different from the traditional definition of rheological conversion [6], $\beta_{\text{rheo}} = (X(t) - X_0)/(X_\infty - X_0)$, where X could be any measured rheological quantity, such as shear viscosity and dynamic modulus. Rheological conversion is quite different from the chemical conversion [23] since it is implicitly assumed that the conversion of reactions varies linearly with the rheological properties. Whereas, the relative conversion defined by Eq. (12) only depends on the assumption of logarithmic addition of viscosity, and can be more accurate in describing the polymer reactions. The equilibrium torque of linear PE under different flow condition $\tau_L(T)$, can be experimentally determined by Haake mixer, and the results are shown in Fig. 5. From Fig. 5, the $\tau_L(T)$ at a specific rotational speed and temperature can be obtained. The torque under the same rotational speed but different temperature can be obtained by using the Arrhenius equation.

It should be noted about the presumption of the conversion based on Eq. (12). It is assumed that the torque of internal

mixer is completely determined by the composition of linear and branched polymers in melt state. This means only the increasing part of the torque after the feeding peak can be related to the chemical reactions. Therefore, the obtained relative conversion will not start from zero at the time when the torque starts to increase. This is attributed to certain radical reaction during the melting of polymer particles, and small amount of branched PE could not lead to a sufficient rise in the torque. The conversion–time curves are presented in Fig. 6. It is seen that the initial conversions are about 30–40%, which means about one-third reaction process happens during the melting of polymer particles. Moreover, the reaction time decreases as the rotational speed increases, which manifests the acceleration of reaction between polymers by stronger flow field.

3.3. Apparent reaction rate parameter k_t

It was known that in diffusion-controlled polymer reactions, the effective rate constant of reaction is usually no longer a constant and becomes dependent on the flow field [5,6,8,24,25]. The diffusion dynamics of polymers start to strongly correlate with its conformation under flow field. Therefore, the reaction rate parameter could be different for polymer chains with different length. Moreover, in a processing flow field like that in an internal mixer or a twin screw extruder, the type and strength of flow field are different everywhere in the mixing chamber, which implies the reaction kinetic parameter could also depend on spatial positions. This makes the problem rather complex. Actually, to simplify the problem, it is reasonable to ignore the dependence of kinetic parameter on the chain length polydispersity, and assume the kinetic parameter to be the same inside the mixing chamber. Although the effect of average kinetic rate parameter differed from the real situation in the mixer, this approach is proved in the next section to be a quite close approximation to describe the polymer–polymer reaction in a strong complex flow. Under such assumption, it is possible to determine the shear rate dependent reaction kinetic parameter by comparing the theoretical conversion with that obtained experimentally. In theory, the reaction conversion is defined as the ratio of current generated branched chains to theoretical yield of them:

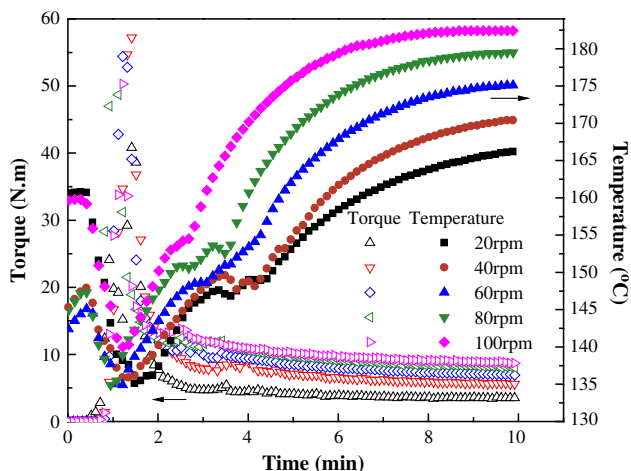


Fig. 5. Temperature and torque curves under different rotor speeds during melt mixing of linear PE in Haake mixer.

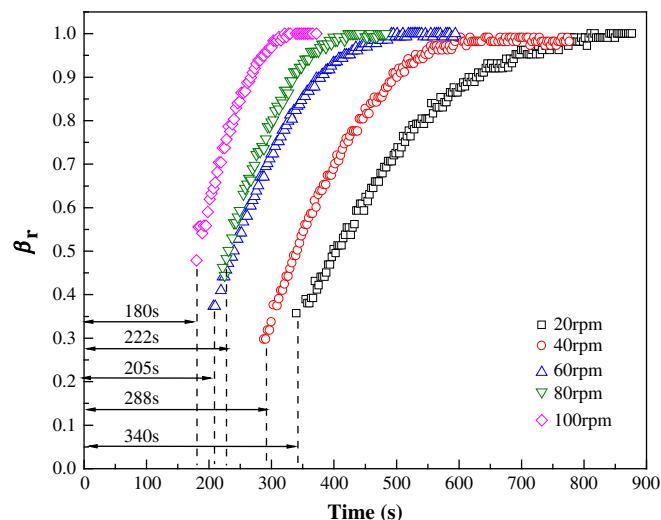


Fig. 6. Reaction conversion obtained from torque of internal mixer against the rotational speed.

$$\beta_{\text{sim}} = \frac{\bar{Y}}{f[I_0]} = \frac{\rho y / 2M_L}{f[I_0]} \quad (13)$$

where \bar{Y} stands for molar concentration of produced branch PE, ρ is density, M_L is the molecular weight of linear PE.

Considering the nonisothermal nature of entire reaction, Arrhenius-type temperature law for k_d and k_t are included, i.e., $k_d = k_d(T_r) \exp[(E_d/R) \cdot (T - T_r/TT_r)]$ and $k_t = k_t(T_r) \exp[(E_t/R) \cdot (T - T_r/TT_r)]$, T_r are reference temperature, E_d is the activation energy of peroxide decomposition reaction, 150 kJ/mol. The activation energy E_t of combination reaction rate constant k_t is taken as 20 kJ/mol referring to polymerization reaction [26] due to the similar kinetic process. Reaction kinetic Eqs. (3), (7), (8) can be solved with proper initial conditions and the experimentally recorded melt temperature. Time dependent concentration of different species like $[I]$, $[P]$, $[P^*]$, $[P-P]$, and β_{sim} can be obtained. Theoretical conversion β_{sim} can be compared with the experimentally determined conversion β_r , and suitable k_t is chosen to minimize the relative error between β_{sim} and β_r . The theoretical conversion curves under five rotational speeds were finally obtained with a list of fitting parameter k_t (see Fig. 7). It can be seen that the chemical kinetic model can fit the reaction process well, especially in the later stage of reaction. These fitted k_t were considered to represent a good approximation to the actual k_t , although the model fittings are a little bit lower than the experimental results in all cases, particularly when the rotational speed is high. It is apparent that the reaction rate parameter k_t depends on the rotational speed of rotor. The higher the rotational speed, the faster the polymer reactions. To correlate the apparent reaction rate parameter with the strength of flow field, the distribution of shear rate inside the mixing chamber is simulated with Fluent under different rotational speeds. A typical two-dimensional computation result of 60 rpm is given in Fig. 8. It is shown that the high shear rate zones are located in nip areas between rotor and cavity wall, and shear rate decreases gradually away from the outer wall of mixer. The volume-weighted average shear rate in the whole cavity can be obtained from Eq. (14) and is listed in Table 2.

$$\bar{\dot{\gamma}} = \frac{1}{V} \int \dot{\gamma} dV \quad (14)$$

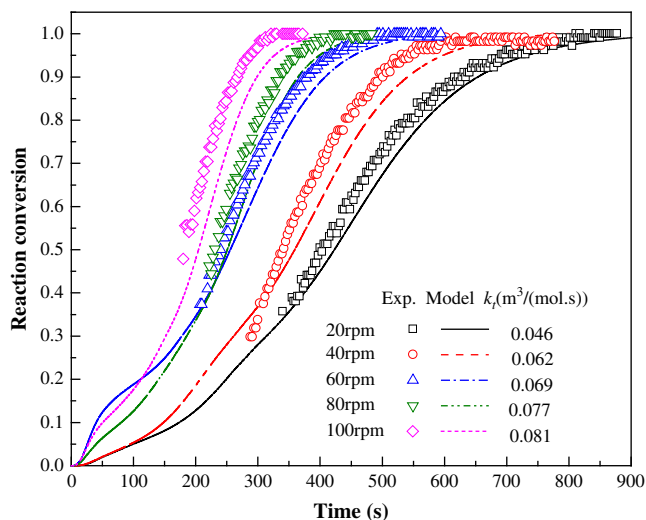


Fig. 7. Best fitting results of k_t through quiescent numerical simulation against the rotational speed.

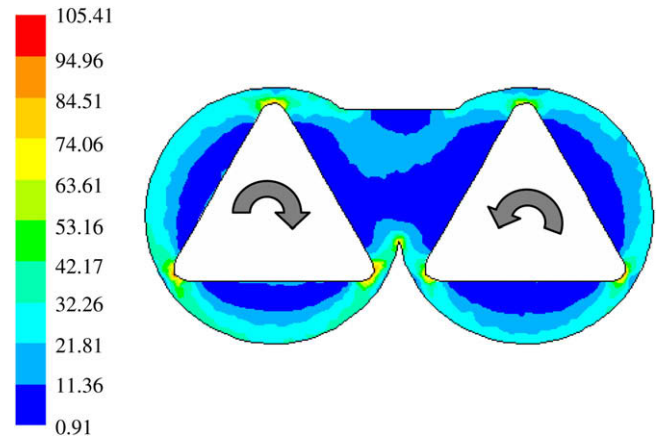


Fig. 8. Shear rate distribution of mixer with left roller rotating at 60 rpm s^{-1} .

Consequently, a scale expression between the combination reaction rate parameter and the average shear rate can be obtained. The $k_t \sim \bar{\dot{\gamma}}$ fitting curve is given in Fig. 9 and the resultant equation is:

$$k_t = 0.0147 \left[1 + (1.21 \bar{\dot{\gamma}})^{0.44} \right] \quad (15)$$

It can be seen that k_t will increase with the shear rate. Under quiescent condition, the kinetic parameter k_t becomes its static value (0.0147 $m^3/(mol \cdot s)$). Eq. (15) can be expressed as a function of the Deborah number, $De = \tau_d \dot{\gamma}$, where τ_d is the characteristic relaxation time. Rheokinetic equation expressed in Deborah number helps to correlate the reaction kinetics with the elasticity of polymers. During the reaction of PE, the relaxation time will change due to the formation of long chain branched PE molecules. The relaxation time of linear and branched PE sample can be determined from the weighted relaxation spectrum (Fig. 10), which is calculated from dynamic modulus (G' and G'') data by GENEREG program [27]. The characteristic relaxation time for pure linear PE chain is about $\lambda_1 = 0.17$ s. For sample modified with DCP, it exhibited an additional longer characteristic relaxation time at $\lambda_2 = 6.2$ s, which is ascribed to the relaxation of branched chains. If the relaxation time of linear chain λ_1 is used to define De , the rheokinetic equation can be written as:

$$k_t = 0.0147 \left(1 + 2.372 De^{0.44} \right) \quad (16a)$$

It is seen that Eq. (16a) is similar to the one obtained theoretically by Fredrickson et al. (Eq. (1a)). The exponent of De is found in our experiments to be 0.44, which is quite close to the theoretical value 0.5. Some difference lies in the coefficient before De . Experimental value (2.372) seems to be larger than the theoretical one (0.8068). However, this value depends on the choice of the characteristic relaxation time. If the relaxation time is chosen as 0.61 s, a value between λ_1 and λ_2 , the coefficient becomes nearly identical to the theoretical value. It should be noticed that the range of average Deborah number in experiments is from 0.89 to 4.4. This range of value is larger than the

Table 2

Volume-weighted averaged shear rate within mixer versus revolution speed of rotor.

Rotational speed (rpm)	20	40	60	80	100
$\bar{\dot{\gamma}}$ (s^{-1})	5.22	10.43	15.67	20.85	26
$\dot{\gamma}_{\text{max}}$ (s^{-1})	36.3	64.3	105.4	173.3	185.6

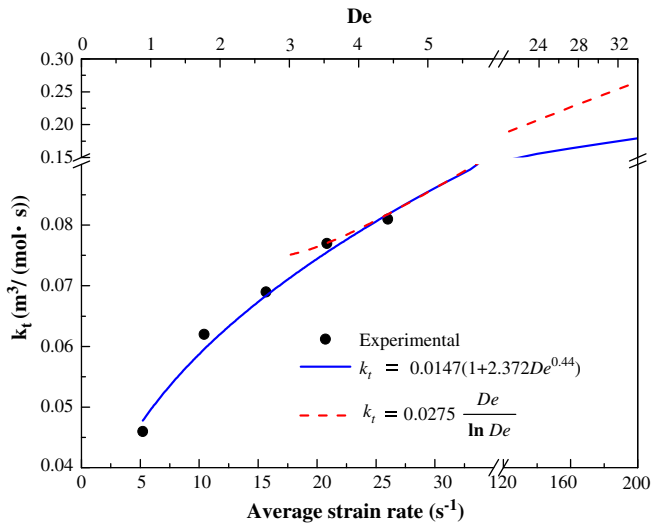


Fig. 9. Effect of flow field on combination reaction kinetic rate constant of HDPE branch reaction in internal mixer.

theoretical requirement for Eq. (1a), i.e., $De \ll 1$. Actually, the experimental range lies in the transition regime from weak convection flow to strong convection flow. The higher part of the experimental result can also be fitted as

$$k_t = 0.0275 \frac{De}{\ln De} \quad (16b)$$

The transition from weak convection to strong convection, i.e., from Eq. (16a) to Eq. (16b), appears at $De \approx 3-4$. The regime for extreme strong shear flow (Eq. (1c)) cannot be accessed by the present experiments, and will not be discussed here.

Another point about the rheokinetic equation is that only the average Deborah number is considered. In fact, the shear rate takes a wide range of distribution inside the mixing chamber (Fig. 8), where the maximum shear rate can be much larger than the average value (Table 2). It is expected that the actual reaction should be faster than that predicted only by the kinetic equation. This is consistent with the observation that the fitted conversions are generally smaller than the experimental values (Fig. 7). Therefore, it is necessary to find out if the rheokinetic equations, Eq. (16a) and (16b), are still valid at stronger flow field. To do such kind of

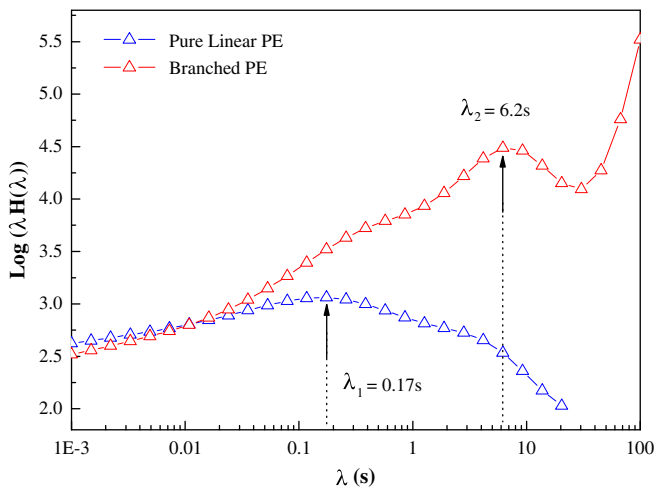


Fig. 10. Weighed relaxation spectrum for linear PE and branched PE at 180 °C.

justification, numerical simulations including convective effects have been presented.

3.4. Numerical simulations on reactive processing

In the reactive processing, the rheokinetic equation determines the effect of strain rate on the reaction rate. However, the actual polymer reaction in mixer will be strongly affected by the spatial feature as well as the convective behavior of flow in the mixer. Therefore, the kinetic equations (Eqs. (3), (7) and (8)) should be replaced by those with convective terms:

$$\frac{\partial [I]}{\partial t} + \mathbf{u} \cdot \nabla [I] = -fk_d(T)[I] + \nabla \cdot (D_I \nabla [I]) \quad (17)$$

$$\frac{\partial [P^*]}{\partial t} + \mathbf{u} \cdot \nabla [P^*] = 2fk_d(T)[I] - k_t(T, \dot{\gamma})[P^*]^2 + \nabla \cdot (D_{P^*} \nabla [P^*]) \quad (18)$$

$$\frac{\partial [P-P]}{\partial t} + \mathbf{u} \cdot \nabla [P-P] = \frac{1}{2}k_t(T, \dot{\gamma})[P^*]^2 + \nabla \cdot (D_{P-P} \nabla [P-P]) \quad (19)$$

where $k_d(T)$ and $k_t(T, \dot{\gamma})$ are both temperature dependent variables, D stands for the diffusion coefficient and is taken as $10^{-23} \text{ m}^2/\text{s}$ for each macromolecule component [28] except for the small molecule DCP whose diffusion coefficient is referenced as $10^{-13} \text{ m}^2/\text{s}$ [29]. Through Eq. (17)–(19), the concentration of initiator, macromolecular radical and branch macromolecule can be convected by the velocity field \mathbf{u} , which can be obtained from the continuity equation and the momentum conservation equation:

$$\nabla \cdot \mathbf{u} = 0 \quad (20)$$

$$\rho \left(\frac{\partial \mathbf{u}}{\partial t} + \mathbf{u} \cdot \nabla \mathbf{u} \right) = -\nabla p + \eta \nabla^2 \mathbf{u} + \rho \mathbf{g} \quad (21)$$

where ρ and η are density and viscosity, respectively, \mathbf{g} is the acceleration of gravity. The viscous heating and the temperature dependent kinetics can be considered by the energy conservation equation:

$$\rho c_v \frac{\partial T}{\partial t} + \rho c_v \mathbf{u} \cdot \nabla T = -\nabla \cdot (k \nabla T) + \tau : \nabla \mathbf{u} \quad (22)$$

where c_v is the volumetric heat capacity, k is the heat conductivity, τ is the stress tensor. Considering little difference of c_v and k between linear and branch PE molecule after reaction, both $c_v = 1850 \text{ J}/(\text{kg K})$ and $k = 0.182 \text{ W}/(\text{m K})$ [30] for pure linear PE will be used in thermal simulation. The two terms on the right hand side of Eq. (22) represent energy transfer due to heat conduction and viscous dissipation, respectively. The chemical reaction enthalpy during branch reaction is neglected due to the dominating heat production by viscous dissipation.

According to previous kinetic assumptions and simplifications, the viscosity expression of blend can be given by [31]

$$\eta_t = \eta_L \left(\frac{M_L}{M_C} \right)^{-3y} \exp \left[\alpha y \left(\frac{M_L}{M_C} - 1 \right) \right] \quad (23)$$

where M_C is the molecular weight at the onset of entanglements for PE macromolecule, $M_C \approx M_e$ (M_e is the average molecular weight between entanglement points), and M_C is about 4000 for PE, η_C is the melt viscosity at the entanglement crossover where $M_L = M_C$. The viscosity η_L actually points to the zero shear viscosity but here a viscosity law combining the Bird–Carreau model of linear PE at 180 °C with Arrhenius temperature function will be adopted. The expression is:

$$\eta_L = 1981.4 \left(1 + (4.76\dot{\gamma})^2\right)^{-0.095} \exp\left(\frac{E_L \cdot T_r - T}{R \cdot T T_r}\right) \quad (24)$$

Besides in Eq. (23), $\alpha = 0.43$ [19] ~ 0.60 [32,33] experimentally and $\alpha = 15/8$ [31] theoretically, but $\alpha = 0.81$ is finally chosen for our system through comparing the zero shear viscosity of reacted product from experimental determination with theoretical prediction of Eq. (23) at different mixing time.

The conservation equations, Eqs. (20)–(22), the rheokinetic equation, Eq. (15), and the constitutive equation, Eq. (23), form a closed model system, which can be solved simultaneously to track the reaction process during mixing. Fluent package was used to simulate the flow and transport process of PE branch reaction.

A typical result for the mass fraction distribution of each reactant/product inside mixer chamber is shown in Fig. 11. It is found that high concentration zone of branch PE generally appears near the outer wall of mixer, the high shear rate zone in the mixer (see Fig. 8). Due to the reaction and mixing process almost occur simultaneously, a maximum of 3.5% mass fraction divergence about branch PE is found within mixer chamber. The radical has a nearly reverse concentration distribution with respect to branch PE. The concentration of residual PE and DCP is mainly related to temperature condition. There is a higher temperature distribution in left half cavity than in right half cavity of mixer because of higher revolution speed of left rotor. Therefore, a similar concentration profile about residual PE and DCP is observed in Fig. 11 where PE and DCP are more consumed in left chamber than in right chamber of mixer.

The simulated reaction conversion for 80 rpm and 100 rpm are given in Fig. 12. The given conversion was also a volume average similar to the average shear rate defined in Eq. (14). It can be seen the computed conversion incorporating the shear rate dependant k_t was higher than the constant k_t case, and is closer to the experimental results. It is proved that a flow field determined k_t

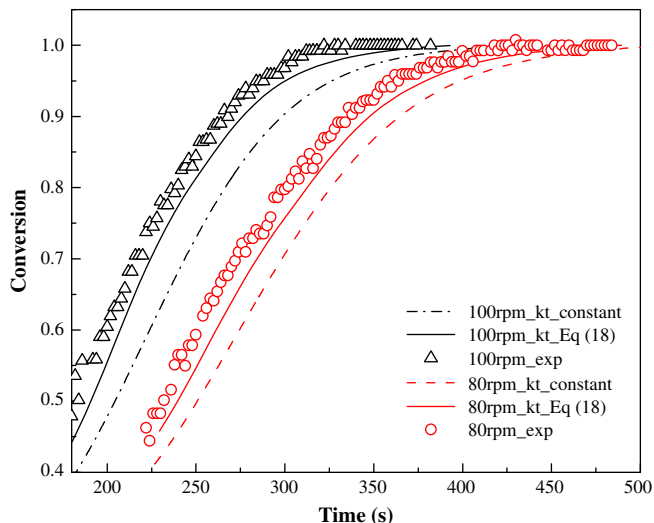


Fig. 12. Comparison of conversion among three cases: experimental, independent kinetic rate constant and shear rate dependent kinetic rate constant.

distribution should and must be considered in the diffusion-controlled polymer reactive processing.

It should be noted that the diffusion coefficient adopted for either macromolecule or small molecule initiator here has almost no influence on the numerical simulation results. It can be explained as follows. Firstly, from the macroscopic point of view, the flow field in the mixer is convection dominated when comparing the convection rate and the diffusion rate. Change in diffusion coefficient will have little effect on the mass transfer and mass distribution inside the chamber. This means the diffusion of components, both initiator and polymer long chains, will not affect macroscopic distribution of components, which is

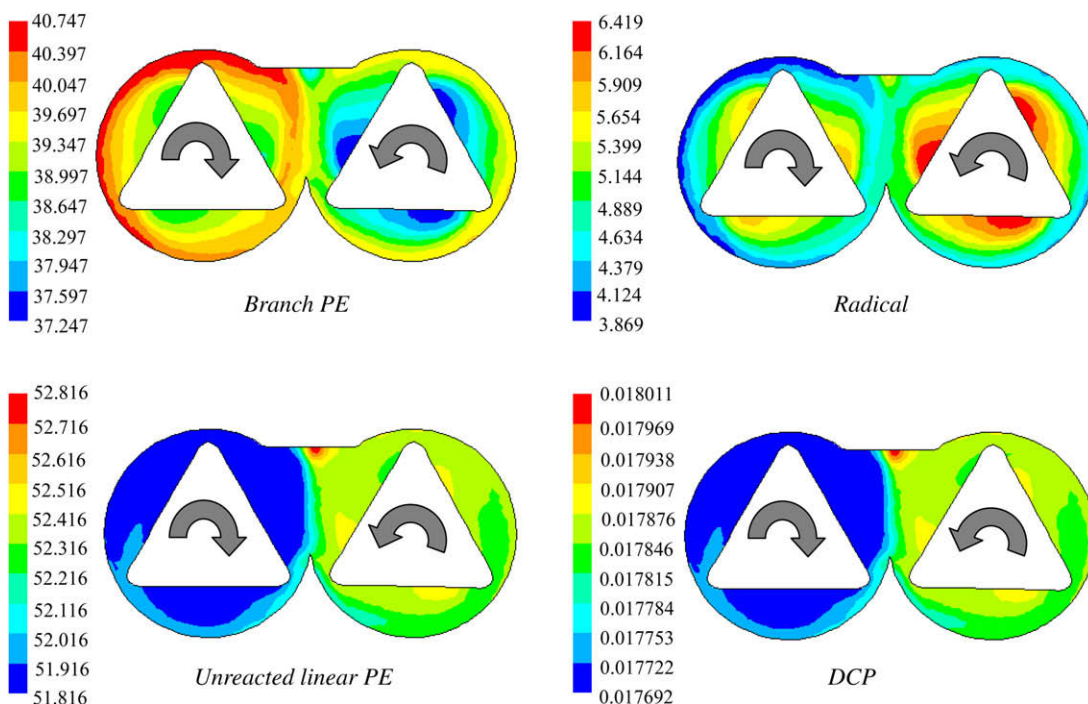


Fig. 11. Mass fraction (%) profile of species when reactive processing for $t = 300$ s under 80 rpm of mixer.

mainly controlled by the strength of convection. Secondly, from the microscopic point of view, diffusion of polymer chains under flow field is believed to affect the reactions between polymers. The theory suggested by Fredrickson et al. gives a prediction about the effect of flow field on the reaction kinetics from the assumption of diffusion-controlled process. However, this effect cannot be simulated directly in macroscopic scale. Both the model and the simulation in this work reflect the apparent kinetics which fit the experiments best. The result on kinetic parameter agrees with the prediction of Fredrickson et al.'s theory, which implies the diffusion-controlled microscopic kinetics could be a reasonable explanation for the effect of flow field on polymer reactions.

Finally, some comments should be made on the rheokinetic equation. Theoretical analysis by Fredrickson et al. was based on many assumptions. Only the reactions between chain end-groups are considered. The free radical reaction in this work, however, happens almost randomly between mid-chain or end-chain sites. But this seems to be not crucial since reaction happens when the reactive sites are close enough (distance smaller than the capture radius, which is believed to be an order of radius of gyration). Moreover, the change of materials properties during reaction is not considered in theory, but really happens in reactive processing. This effect is somehow difficult to evaluate since it could be coupled with the effect of varying flow field inside the mixer. Although there exists some limitations on the theoretical analysis [4], the polymer reactions can be well described by the corresponding rheokinetic equations.

4. Conclusion

The rheokinetic study on homogeneous polymer reactions in melt state under strong flow field was carried out. High density polyethylene molten branching process initiated by Dicumyl peroxide was chosen as reactive system in an internal batch mixer. A new defined reaction conversion was used to extract the apparent reaction kinetic parameter under different flow conditions. The correlation between the apparent kinetic parameter and the Deborah number has a very good agreement with the theoretical analysis by Fredrickson and Leibler. This relationship was further verified by a numerical simulation on reactive processing of PE branching in the internal mixer. The simulation results revealed

that the flow effects on polymer reactions should not be ignored in real polymer processing. The diffusion-controlled rheokinetic theory presented by Fredrickson and Leibler was verified experimentally for the first time, and it works quite well in the actual polymer reactive processing although there were still some underlying assumptions in the theory.

Acknowledgements

The authors are thankful for the financial support for this work from the National Natural Science Foundation of China (Grant No. 50390095).

References

- [1] O'Shaughnessy B, Vavylonis D. *Macromolecules* 1999;32(6):1785–96.
- [2] Liu MG, Yu W, Zhou CX. *J Appl Polym Sci* 2006;100(1):839–42.
- [3] de Gennes PG. *J Chem Phys* 1982;76(6):3316–26.
- [4] Fredrickson GH, Leibler L. *Macromolecules* 1996;29(7):2674–85.
- [5] Liu MG, Yu W, Zhou CX. *Chin J Polym Sci* 2006;24(2):135–8.
- [6] Malkin AYA, Kulichikhin SG. *Polym Eng Sci* 1997;37(8):1322–30.
- [7] Lee JK, Gillham JK. *J Appl Polym Sci* 2003;90(10):2665–75.
- [8] Han IS, Chung CB, Lee JW. *Rubber Chem Technol* 2000;73(1):101–13.
- [9] Cioffi M, Hoffmann AC, Janssen LPBM. *Polym Eng Sci* 2001;41(3):595–602.
- [10] Kale LT, O'Driscoll KF. *Polym Eng Sci* 1982;22(7):402–9.
- [11] Liu MG, Zhou CX, Yu W. *Polym Eng Sci* 2005;45(4):560–7.
- [12] Liu JY, Yu W, Zhou CX. *Polymer* 2006;47(20):7051–9.
- [13] Liu JY, Yu W, Zhou CX. *Polymer* 2008;49(1):268–77.
- [14] Liu JY, Yu W, Zhou CX. *Polymer* 2009;50(2):547–52.
- [15] *Dynamic Mesh Theory, Fluent 6.3 Documentation* 11.3; 2006.
- [16] Yamazaki T, Seguchi T. *J Polym Sci Part A Polym Chem* 1997;35(2):279–84.
- [17] Dorn M. *Adv Polym Tech* 1985;5(2):87–97.
- [18] Bousmina M, Ait-Kadi A, Faisant JB. *J Rheol* 1999;43(2):415–33.
- [19] Struglinski MJ, Graessley WW. *Macromolecules* 1988;21(3):783–9.
- [20] Tsenoglou C. *Macromolecules* 1991;24(8):1762–7.
- [21] Haley JC, Lodge TP. *J Rheol* 2004;48(2):463–86.
- [22] Liu CY, Wang J, He JS. *Polymer* 2002;43(13):3811–8.
- [23] Liu MG, Yu W, Zhou CX, Yin JH. *Polymer* 2005;46(18):7605–11.
- [24] Malkin AYA. *Polym Eng Sci* 1980;20(15):1035–44.
- [25] Kulichikhin SG, Malkin AYA, Polushkina OM, Kulichikhin VG. *Polym Eng Sci* 1997;37(8):1331–8.
- [26] Pan Z. *Polymer chemistry*. 2nd ed. Beijing: Chemical Industry Press; 1997. p. 41.
- [27] Roths T, Marth M, Weese J, Honerkamp J. *Comput Phys Commun* 2001; 139(3):279–96.
- [28] Qiu H, Bousmina M. *J Rheol* 1999;43(3):551–67.
- [29] Ni XY, Sun XH, Ceng D. *Polym Eng Sci* 2001;41(8):1440–7.
- [30] Bai Y, Sundararaj U, Nandakumar K. *ANTEC* 2004;3:2793–7.
- [31] Tsenoglou CJ, Gotsis AD. *Macromolecules* 2001;34(14):4685–7.
- [32] Ball RC, McLeish TCB. *Macromolecules* 1989;22(4):1911–3.
- [33] Milner ST, McLeish TCB. *Macromolecules* 1997;30(7):2159–66.